Journal of Inflammation Research

Dovepress
Taylor & Francis Group

Open Access Full Text Article

ORIGINAL RESEARCH

Role and Mechanism of Mitochondrial Ribosomal Proteins in Septic Myocardial Injury

Liuli Wu[1,*], Junchao Huang[2,*], Xiongfei Jia[3], Xiaoqin Mao[1]

[1]Department of Clinical Laboratory, The First People's Hospital of Yunnan Province, The Affiliated Hospital of Kunming University of Science and Technology, Kunming, Yunnan, 650500, People's Republic of China; [2]Department of Clinical Laboratory, Yunnan New Kunhua Hospital, Kunming, Yunnan, 650000, People's Republic of China; [3]Department of Clinical Laboratory, 920th Hospital of Joint Logistics Support Force of Chinese People's Liberation Army, Kunming, Yunnan, 650000, People's Republic of China

*These authors contributed equally to this work

Correspondence: Xiaoqin Mao, Department of Clinical Laboratory, The First People's Hospital of Yunnan Province, The Affiliated Hospital of Kunming University of Science and Technology, Kunming, Yunnan, 650500, People's Republic of China, Email maoxq_123@163.com; Xiongfei Jia, Department of Clinical Laboratory, 920th Hospital of Joint Logistics Support Force of Chinese People's Liberation Army, Kunming, Yunnan, 650000, People's Republic of China, Email saoscm@163.com

Objective: To investigate the role of mitochondrial ribosomal proteins (MRPs) in the pathogenesis and progression of septic myocardial injury. Additionally, we aim to propose new technical strategies and experimental foundations for the prevention and treatment of septic myocardial injury.

Methods: Animal and cell models of septic myocardial injury were established. Aberrantly expressed MRPs were screened using transcriptome sequencing, and their expression was verified by RT-qPCR and Western blot. Subsequently, overexpressed and knock-down cell models of myocardial injury were constructed. The effects on CO I, PGC-1α, ATP content, ROS fluorescence intensity, mitochondrial membrane potential, and GSDMD were assessed, along with changes in caspase-4 and IL-1β expression levels.

Results: Transcriptome sequencing revealed a reduction in MRPs expression in mice with septic myocardial injury. Both RT-qPCR and Western blot analysis confirmed the decreased expression of MRPs in animal and cell models of septic myocardial injury. Furthermore, overexpression of both MRPS16 and MRPL47 mitigated the decrease in CO I and PGC-1α levels induced by septic myocardial injury. Additionally, overexpression of MRPS16 and MRPL47 alleviated the elevated levels of IL-1β, caspase-4, and GSDMD caused by septic myocardial injury.

Conclusion: The findings suggest that both MRPS16 and MRPL47 can mitigate mitochondrial injury by attenuating mitochondrial biosynthesis dysfunction, energy metabolism disorders, and Ca^{2+} disturbances caused by septic myocardial injury. This ultimately reduces cellular damage and alleviates septic myocardial injury.

Keywords: septic myocardial injury, MRPS16, MRPL47, mitochondrial function

Introduction

Sepsis is a systemic inflammatory response caused by the invasion of an organism by a pathogen such as a bacterium, fungus, or virus.[1] According to statistics, sepsis affects more than 40 million people worldwide each year, and more than 11 million of them die from sepsis, with a mortality rate of over 25%.[2] The heart is particularly vulnerable to damage from sepsis. The incidence of septic myocardial injury is approximately 40%, with a mortality rate ranging from 70% to 90%.[3] Septic myocardial injury leads to weakening of the heart, often manifested as dilatation of the right and left ventricles, reduction in left ventricular ejection fraction, and myocardial systolic and diastolic dysfunction. These changes result in decreased pumping function of the heart, leading to systemic blood circulation disorders and inadequate organ perfusion,[4,5] exacerbating the patient's condition and significantly impacting the prognosis for sepsis patients while increasing their risk of mortality.[6] The mechanisms underlying septic myocardial injury are highly complex and primarily involve excessive cardiac inflammation response, energy metabolism dysfunction, mitochondrial damage, oxidative stress, cell apoptosis, pyroptosis, and ferroptosis.[7–9] Mitochondria play crucial roles in energy production as well as

Received: 23 September 2024
Accepted: 6 January 2025
Published: 21 February 2025

various cellular functions including calcium signaling, redox homeostasis, and apoptosis. Mitochondrial dysfunction is mainly characterized by (1) decreased ATP synthesis, (2) increased ROS, (3) Ca^{2+} disorder, and (4) cell death.[10–12] Additionally, mitochondria regulate intracellular calcium homeostasis, the activity of calcium-sensitive enzymes, and play an important role in Ca^{2+} signaling.

More than 80 mitochondrial ribosomal proteins (MRPs) have been identified in mammals, all of which are encoded by nuclear genes and synthesized in the cytoplasm. They are then directionally translocated into the mitochondria to assemble with rRNA and form mitochondrial ribosomes.[13] Based on their function and location, they are categorized into large subunit proteins MRPL and small subunit proteins MRPS. Cardiomyocytes contain the largest number of mitochondria, accounting for approximately 30% of their volume.[14] Mitochondria with normal MRPs expression play a crucial role in maintaining cardiac function. Dysregulation of MRPs expression leads to mitochondrial translation disorders and respiratory chain damage, resulting in cell metabolic disorders.[15] For instance, the absence of MRPL10 decreases mitochondrial activity and affects mitochondrial complex expression, impacting both mitochondrial function and the cell cycle.[16] Low expression of MRPS28 affects the translational function of mitochondrial ribosomes. Mutation of MRPS34 impairs protein synthesis and leads to mitochondrial dysfunction,[17] disrupting the stability of mitochondrial ribosomal small subunits and affecting the translation of mitochondrial proteins, ultimately causing Leigh syndrome.[18] Mutations in MRPS16[19] and MRPS22[20] have also been shown to result in defects in the mitochondrial respiratory chain. Numerous studies have demonstrated aberrant expression of MRPs in tumors as well. For example, MRPS6,[21] MRPS30,[22] MRPS12, and MRPL13[23] play critical roles in breast cancer. Studies on the relationship between MRPs and gastrointestinal tumors have also yielded significant findings, such as with MRP18-A,[24] MRL38, and liver cancer.[25] High expression of MRPS23 has been found to result in mitochondrial dysfunction, proliferation of hepatocellular carcinoma, and poor survival outcomes.[26] Additionally, several studies have demonstrated that aberrant expression of MRPs can lead to heart disease, including hypertrophic cardiomyopathy and thrombosis.[27,28] Myocardial hypertrophy and thrombosis are among the pathologic changes in the development of septic heart failure. A study also identified a variant of MRPS14 as a cause of perinatal hypertrophic cardiomyopathy,[29] while mutation in MRPL44 is an important factor in the development of mitochondrial cardiomyopathy in human infants.[30] Pathogenic mutations in MRPL3 have been linked to the clinical phenotype of combined oxidative phosphorylation defect-9 (COXPD-9), with severe hypertrophic cardiomyopathy being the predominant manifestation following mutations in the gene.[31] Furthermore, MRPL16 has been significantly associated with infectious cardiomyopathy,[32] while MRPL12 plays a role in homeostatic regulation of mitochondrial transcription and ribosome biogenesis.[33] Lastly, it has been observed that expression levels of MRPS21, MRPS2, and MRPL50 are upregulated in cardiac hypertrophic cells, whereas expression level of MRPL34 is downregulated.

However, the role and mechanism of mitochondrial ribosomal proteins (MRPs) in septic myocardial injury have not been previously reported. Therefore, this study aims to investigate the role and mechanism of MRPs in septic myocardial injury. By focusing on MRPS16 and MRPL47 as the research entry point, we utilized cell transfection and other experimental techniques to examine the effects of MRPs on mitochondrial function and cell death mode. Additionally, we explored the role and molecular mechanism of MRPs in septic myocardial injury. This research aims to provide a new technological strategy and experimental basis for preventing and treating septic evidence of myocardial injury, as well as serving as an experimental foundation for the development of new drugs.

Materials and Methods

Establishment of a Murine Model for Septic Myocardial Injury

The LPS model, as one of the classical models, has an extremely wide application in the field of sepsis research.[34] Ten male C57BL/6J mice, aged 6–8 weeks and weighing approximately 20g, with SPF grade (Animal Qualification Certificate No. SYXK (Yunnan) K2021-0005), purchased for Experimental Animal Center, Kunming Medical University, were selected and randomly assigned to two groups: the control group (Control group) and the experimental group (LPS group). After a 2-week acclimatization period, mice in the LPS group were intraperitoneally injected with a 10 mg/kg LPS solution, while mice in the Control group received an equal volume of PBS solution via intraperitoneal

injection. The condition of the mice was regularly monitored. After 24 hours of LPS treatment, blood was collected by removing the eyes of the mice to obtain serum for inflammation and injury marker detection. The hearts of the mice were then collected, washed in 0.9% NaCl solution, dried, and preserved; a portion was fixed in 4% paraformaldehyde for HE staining, while another portion was stored at −80°C. Transcriptome sequencing was conducted to identify MRPs genes with abnormal expression levels which were subsequently validated using RT-qPCR and Western blotting techniques (Ethics No.920IEC/AF/61/2021-01.1).

Construction of a Cell Model for Septic Myocardial Injury

AC16 cells (purchased from BeNa Culture Collection, cell number BNCC339980) were divided into two groups: the control group and the experimental group. In the experimental group, AC16 cardiomyocytes were treated with LPS and Nigericin; while in the control group, cells continued to be cultured in 37°C, 5% CO_2 medium. Nigericin is an antibiotic that acts in combination with LPS, thereby inducing an inflammatory response in cells. Cell viability was assessed using CCK8, and inflammatory factors as well as myocardial injury markers were measured to evaluate the extent of cell injury. Subsequently, significantly different MRPs were identified for further functional and mechanistic studies. Septic myocardial injury cell models with overexpression and knockdown of MRPs were constructed. The effects of overexpression and knockdown were confirmed through RT-qPCR and Western blot analysis. Mitochondrial function tests included measuring mitochondrial biosynthesis by assessing the expression levels of Cytochrome C Oxidase Subunit I (CO I) and PGC-1α (peroxisome proliferator-activated receptor-γ coactivator-1α), which is a key regulator of mitochondrial biosynthesis; evaluating energy metabolism disorders by detecting ATP content and ROS fluorescence intensity; as well as assessing Ca^{2+} disorder through measurement of mitochondrial membrane potential (MMP) using TMRE staining. Focal death assays involved Western blot analysis for GSDMD and caspase-4, along with RT-qPCR for IL-1β.

HE Staining of Heart Tissue

Mice hearts were collected after cervical dislocation execution, washed in 0.9% sodium chloride solution, partially preserved in 4% paraformaldehyde fixative, dehydrated, hyalinized, wax-dipped, and embedded before sectioning and staining. After sealing, the sections were microscopically observed and photographed.

ELISA for Measurement of Inflammatory Factors in Mouse Serum

After mice were treated with LPS (10 mg/kg) by intraperitoneal injection for 24h, blood was extracted from the eyeballs of mice and serum was separated for the detection of myocardial injury markers. The serum was collected from different treatment groups, centrifuged at 3500 rpm for 10 min at 4°C, and the supernatant was taken from another clean 1.5 mL EP tube. The mouse ELISA IL-6 kit (EK0411), ELISA IL-1β kit (bsk12015) and ELISA TNF-α kit (EK0527) instructions were used, respectively, and the optical density values of the reaction wells were determined by enzyme labeling instrument and the standard curves were plotted, and then the serum levels of IL-6, IL-1β, and TNF-α in the mouse serum were calculated, respectively. Content of IL-6, IL-1β, and TNF-α in the serum of mice.

Detection of Markers of Myocardial Injury in Mouse Serum and Cell Culture Supernatants

Myocardial injury markers in mouse serum and AC16 cell culture supernatants were detected by mouse ELISA cTnI kit (MM-0791M1), mouse ELISA LDH kit (CSB-E11723m), human ELISA cTnI kit (MM-0922H1), and human ELISA LDH kit (MM-0354H1) respectively, which was operated according to the instructions, and the absorbance value of each reaction well was determined by the enzyme marker. Finally, a standard curve was plotted and the cTnI and LDH levels were calculated.

AC16 Cell Culture

The cryopreservation tube was retrieved and placed in water at 37°C with gentle agitation. After the cells were thawed, the cryopreservation solution was transferred into a centrifuge tube. The tube was centrifuged at 1000 rpm for 5 minutes,

and then the cells were resuspended in the culture medium. 1 mL of the cell suspension was transferred into a new T25 culture flask. Subsequently, 4 mL of DMEM medium supplemented with 10% fetal bovine serum (FBS) was added and mixed thoroughly. The flask was then placed in a 37°C incubator with 5% CO_2 for culturing. When the cell density reached 80–90%, cell passage was carried out. The original culture medium was first discarded, and PBS (BL302A) was added into the flask for rinsing twice. Then, 1 mL of trypsin (25200056) was added to digest the cells. The cell suspension was then transferred into a centrifuge tube, centrifuged at 1000 rpm for 5 minutes, and the supernatant was discarded. The cells were resuspended in the culture medium, aliquoted into new culture flasks, and sufficient culture medium was added to ensure that the cells had adequate nutrition and growth space. After gently shaking the culture flasks, they were placed back into the incubator for further culturing.

CCK8 Assay for Cell Viability

CCK8 assay was performed using the Enhanced CCK8 Kit (BA00208). Cells were inoculated into 96-well culture plates for overnight incubation, and different concentrations of drugs were added to each well to stimulate the cells, which were again put into the incubator for incubation. At the end of incubation, 10 μL of CCK8 solution was added to each well, and the cells were again incubated in a carbon dioxide incubator for about 2 h. The cells were then incubated for about 2 h in a CO_2 incubator. Finally, the absorbance value at 450 nm was measured with an enzyme marker to calculate the survival of cells in each well.

RT-qPCR

Cell samples were extracted with RNA extraction kit (B0004DP). Tissue samples were clipped and lysed by adding 1 mL of Trizol reagent to lysed cells, 200 μL of trichloromethane to extract RNA, 500 μL of isopropanol to precipitate the RNA, and anhydrous ethanol to wash the RNA and then 30 μL of enzyme-free water to solubilize the RNA to extract the RNA. The concentration and purity of the RNA was determined by the RNA Reverse Transcription Kit All in-One First-Strand Synthesis Master Mix (with dsDNase) (EGN). The concentration and purity of RNA were determined using a Nanodrop 2000 spectrophotometer, and the reverse transcription PCR reaction was carried out using the RNA Reverse Transcription Kit All-in-One First-Strand Synthesis Master Mix (with dsDNase) (EG15133S), and the reaction system (20 μL) was as follows: 4 μL All-in-One First-Strand Synthesis Master Mix (with dsDNase) (EG15133S). The reaction system (20 μL) was as follows: 4 μL All-in-One First-Strand Synthesis Master Mix, 1 μL dsDNase, 1 μg of template RNA, and Nucleic-Free Water to make up to 20 μL. The reaction conditions were set as follows: 37°C for 2 min, 55°C for 15 min, and 85°C for 5 min. cDNA was diluted 5-fold, and the reaction conditions were set using Taq SYBR® Green, which is a proprietary biotechnology company of Jiangsu Yugong Bio-technology Co. Ltd Taq SYBR® Green qPCR Premix (Universal) (EG20117M) kit for RT-qPCR reaction. Primers for quantification were designed using Primer-BLAST on the NCBI website (https://www.ncbi.nlm.nih.gov/), and primers were synthesized by Prime Biotech, as shown in Table 1 and Table 2. The RT-qPCR reaction system (20 μL) was configured into a 20 μL reaction system in octuplex tubes as follows: 10 μL Taq SYBR Green qPCR Premix, 0.4 μL upstream primer (10 μM), 0.4 μL downstream primer (10 μM), 2 μL cDNA template, and 7.2 μL enzyme-free water. The reaction conditions were: pre-denaturation at 95°C for 30s; 40 cycles of 95°C for 10s and 60°C for 30s; 60°C for 60s and 95°C for 15s to plot the melting curve.

Western Blot

The tissues and cells were collected into EP tubes, and the configured protein lysis solution (RIPA: protease inhibitor = 1:100 ratio) was added, blown and mixed, and placed on ice for 30 min for protein lysis. Then after centrifugation at 12000 rpm at 4°C for 10 min, the supernatant protein was aspirated to measure the total protein concentration using the enhanced detection kit (P0010) from Shanghai Beyotime, and the 5× protein uploading buffer was configured with the samples to be tested at a ratio of 4:1 according to the protein content, and then mixed and centrifuged and placed into a water bath or metal bath set at 100°C in advance, and then the EP tubes were covered tightly and the protein was The denatured protein was centrifuged and then the protein was sampled for run electrophoresis. The samples were added on 12.5% SDS-PAGE, transferred to a PVDF membrane, closed with skim milk powder and incubated overnight with primary antibody. Primary antibodies against MRPL19 (bs-17775R), MRPL12 (PA5-112178), MRPL49 (bs-17802R),

Table 1 Primer Sequences (Mice)

Primer	Sequences (5′-3′)
GAPDH-F	ATGGTGAAGGTCGGTGTGA
GAPDH-R	AATCTCCACTTTGCCACTGC
IL-1β-F	CTCGCAGCAGCACATCAACAAG
IL-1β-R	CCACGGGAAAGACACAGGTAGC
IL-6-F	AGTTGCCTTCTTGGGACTGA
IL-6-R	TCCACGATTTCCCAGAGAAC
TNF-α-F	CCTCCAGAAAAGACACCA
TNF-α-R	ACAAGCAGGAATGAGAAGAG
MRPL19-F	CATGGCAGAAAGTTGTAGGG
MRPL19-R	TGCTCTGAAATCGGCTTGG
MRPL47-F	TACAACAGGAGGCGGTTCTTC
MRPL47-R	AGGGCGTGTTTCTCAATTCT
MRPL12-F	CTTACCAAGTGAACACACCC
MRPL12-R	AGGTGGTCCTTTATACC
MRPS14-F	GTCCGTGGCGGGAGA
MRPS14-R	TGGCTGAATGCTCTGCT
MRPL3-F	AGCCGTGGCCTTTACATCCCT
MRPL3-R	TCATGCCTAGCTTCAGGGCGA
MRPS16-F	TACCACGGAGGCCACCTAAC
MRPS16-R	AGCAGCCACAATGCGGTAAA
MRPL49-F	CGGCTTTGTGGAGTCTGTGGA
MRPL49-R	AAGTAGGGCAAGCTGGGAAGA
MRPL34-F	ACATCAAGCGCAAGCACAAG
MRPL34-R	CGGCGTCTGAGTCTATTCCC

Table 2 Primer Sequences (Human)

Primer	Sequences (5′-3′)
GAPDH-F	TGACTTCAACAGCGACACCCA
GAPDH-R	CACCCTGTTGCTGTAGCCAAA
IL-1β-F	CCGACCACCACTACAGCAAGG
IL-1β-R	GGGCAGGGAACCAGCATCTTC
TNF-α-F	CCCATGTTGTAGCAAACCCTC
TNF-α-R	TATCTCTCAGCTCCACGCCA
IL-6-F	CAATGAGGAGACTTGCCTGG
IL-6-R	TGGGTCAGGGGTGGTTATTG
MRPL19-F	ACGAGATGCCCTTCCTGAAT
MRPL19-R	GGACGTTCCCAGCGTTTAGA
MRPL12-F	GGAGGACTTGTGTTCAGGGG
MRPL12-R	GCAATTCTCCCAAACGGCTC
MRPL49-F	CCCTCCAGATTACCCCAGGT
MRPL49-R	GGGGATCTGGGATCCTGGTA
MRPL34-F	GGTGTCTAGGGCCTGGAGATG
MRPL34-R	CAAGACAGCCATATCCGCAG
MRPS14-F	GGCAATTCCAAGAGGGCAAC
MRPS14-R	TGACTGGAACCTGAACTCGC
MRPS16-F	GGTCCACCTCACTACTCTCCT
MRPS16-R	CCCTGGGACACTTGTTGTGA

(*Continued*)

https://doi.org/10.2147/JIR.S495987

Table 2 (Continued).

Primer	Sequences (5′-3′)
MRPL47-F	CACAGTGCACAACAGTCCAAA
MRPL47-R	CCAGTGGATTGGTAGAACTGCT
MRPL3-F	AAACTTCCCCACGGCTACTG
MRPL3-R	GGGAAGACTCGACTCACGAC
PGC-1α-F	CCAGGTCAAGATCAAGGTCTCCAG
PGC-1α-R	TGCGTGCGGTGTCTGTAGTG
CO I-F	CCTCTTCGTCTGATCCGTCCTAATC
CO I-R	TGGTGTTGAGGTTGCGGTCTG

MRPL34 (PA5-103525), MRPS14 (PA5-120370), MRPS16 (GTX66585), MRPL47 (PA5-101365), MRPL3 (PA5-106677), caspase-4 (ER62908), GSDMD (ER1901-37), GAPDH (GB15004-100), and β-actin (ab8227) were washed three times with TBST for 10 min each time, and then washed with a 1:5000 dilution at room temperature with the of horseradish peroxidase-coupled secondary antibody for one and a half hours at room temperature, and finally the protein bands were detected by chemiluminescence.

Plasmid Transfection Experiment

The MRPS16 and MRPL47 overexpression and knockdown plasmids in this experiment were designed and synthesized by Shanghai Jikai Gene Biology Co. The overexpression GV657 control vector did not insert any sequence, and the knockdown GV493 control vector inserted a meaningless sequence: TTCTCCGAACGTGTCACGT. Both the over-expression and knockdown vectors had green E-GFP fluorescent protein. The knockdown plasmid was designed with three sh-RNA target sequences RNAi, and the target sequence with the best knockdown effect was selected for subsequent experiments. Tiangen endofree mini plasmid kit (DP118) was used to extract the plasmids. The plasmid was transfected into cells with lipo3000 transfection reagent (L3000015), and the cell infection rate was observed by fluorescence microscope after the transfection reached 24h. The fluorescence rate was ensured to be above 50%, the cell sediment was collected, and RNA and protein were extracted according to the above method, and the overexpression and knockdown effects were evaluated by using RT-qPCR and Western blot experiments.

ATP Kit to Detect ATP in Cardiomyocytes

ATP content of cardiac tissues was measured using ATP assay kit (S0026). The cell samples were first collected, and after adding 200 μL of lysate and blowing repeatedly, the supernatant was centrifuged at 4°C 12000g for 5 minutes. Then the diluted ATP assay working solution was added into the 96-well plate in advance and left at room temperature for 5 min to remove the background ATP. Then the samples and different concentrations of ATP standards (0.01, 0.1, 1 and 10 μM) were added into the reaction wells, mixed well and then placed in the enzyme marker to detect the intracell RLU values of each group of cells and plotted the standard curve, and the ATP content was calculated according to the standard curve.

Detection of ROS in Living Cells by Flow Cytometry

Cells were inoculated into 6-well plates for overnight incubation, transfected for 24h and drug-treated for 24h, then removed and the culture medium was aspirated. DHE staining solution was diluted with serum-free medium at 1:1000 to a final concentration of 10 μM. DHE staining working solution was added to each well to cover the cells, which were incubated in an incubator for 20 min. Trypsin digested the cells, and the cells were resuspended in PBS, and then analyzed and detected the cell ROS using a flow cytometer with an excitation wavelength of 488 nm and an emission wavelength of 578 nm, emitting red fluorescence, and the results were analyzed by using FlowJo software to select FL3 channel.

Mitochondrial Membrane Potential Assay (TMRE Staining)

AC16 cells were inoculated into 6-well plates after transfection and dosing, the culture medium in the 6-well plates was aspirated, washed once with PBS, 100 μL of 50–500 nM TMRE working solution was added to each well, and the cells were incubated in an incubator at 37°C for 5–30 min. At the end of the incubation, the cells were washed twice with culture medium, and 2 mL of the medium was added and placed under a fluorescence microscope to be observed and analyzed, and the excitation wavelength of TMRE was 550 nm and the emission wavelength was 575 nm. Changes in red fluorescence intensity represent the level of mitochondrial membrane potential in cardiomyocytes.

Statistical Analysis

Results were analyzed using SPSS 19.0 and GraphPad Prism 9.0 software. When comparing data between two groups, *t*-tests or rank sum tests were used. One-way ANOVA was used when making comparisons between multiple groups. Data were expressed as mean ± SEM. In particular, for RT-qPCR results, relative expression was calculated using the $2^{-\Delta\Delta Ct}$ method. For Western blot results, Image J software was used to analyze the grayscale values between the samples of the proteins to be tested and the internal reference. For statistical analysis, $P<0.05$ indicated that the difference was significant.

Results

Construction of Septic Myocardial Injury Mouse Model

Firstly, the septic myocardial injury mouse model was constructed. The experimental group was injected intraperitoneally with 10 mg/kg LPS, and the control group was injected intraperitoneally with an equal amount of PBS. 24h later, it was found that the experimental mice had obvious symptoms of septic shock, which were mainly manifested as a drop in body temperature, weakened respiration, slow movement, acanthosis and roughness of the hairs to the touch, the whiteness of the eyeballs, and the appearance of a large amount of white secretion around the eye sockets (Figure 1A). HE staining showed that there was a large number of inflammatory cells exuded between myocardial tissues, some myocardial cells showed vacuolar changes, and the walls of vascular tubes were edematous (Figure 1B). To further verify whether the mouse model of septic myocardial injury was successfully constructed, mouse serum was collected for inflammation and myocardial injury marker assays. ELISA results showed that compared with the control group, the expression levels of IL-6, IL-1β, and TNF-α in the serum of the experimental group of mice were significantly higher (Figure 1C), while the levels of LDH and cTnI in the LPS group were significantly elevated (Figure 1E). RT-qPCR results showed that the expression levels of IL-6, IL-1β and TNF-α mRNA were significantly elevated in the heart tissues of mice in the experimental group, which was consistent with the ELISA results (Figure 1D), indicating that the myocardium had been severely damaged, and an animal model of septic myocardial injury had been successfully established.

Mitochondrial Ribosomal Proteins are Significantly Under-Expressed in Animal Models of Septic Myocardial Injury

After successful modeling, transcriptome sequencing was performed on cardiac tissues of normal control mice and septic myocardial injury model mice, revealing many differentially expressed genes. Among them, MRPs (MRPS14, MRPS16, MRPL3, MRPL12, MRPL19, MRPL34, MRPL47, MRPL49) were downregulated in the LPS group (Figure 2A). To further investigate the biological functions of these differentially expressed genes, GO and KEGG enrichment analyses were conducted separately. In the GO enrichment analysis, differentially expressed genes were found to be involved in ribosomes at the Biological Process (BP), Cell Components (CC), and Molecular Function (MF) levels, and KEGG enrichment analysis also indicated enrichment of ribosomes (Figure 2B).

The sequencing results were further validated using RT-qPCR and Western blot, which showed that the mRNA expression levels of MRPs (MRPS14, MRPS16, MRPL3, MRPL12, MRPL19, MRPL34, MRPL47, MRPL49) in cardiac tissues of the experimental group were significantly decreased compared with those of the control group (Figure 2C) Western blot results showed that protein expression levels of MRPs (MRPS14, MRPS16, MRPL3, MRPL12, MRPL19,

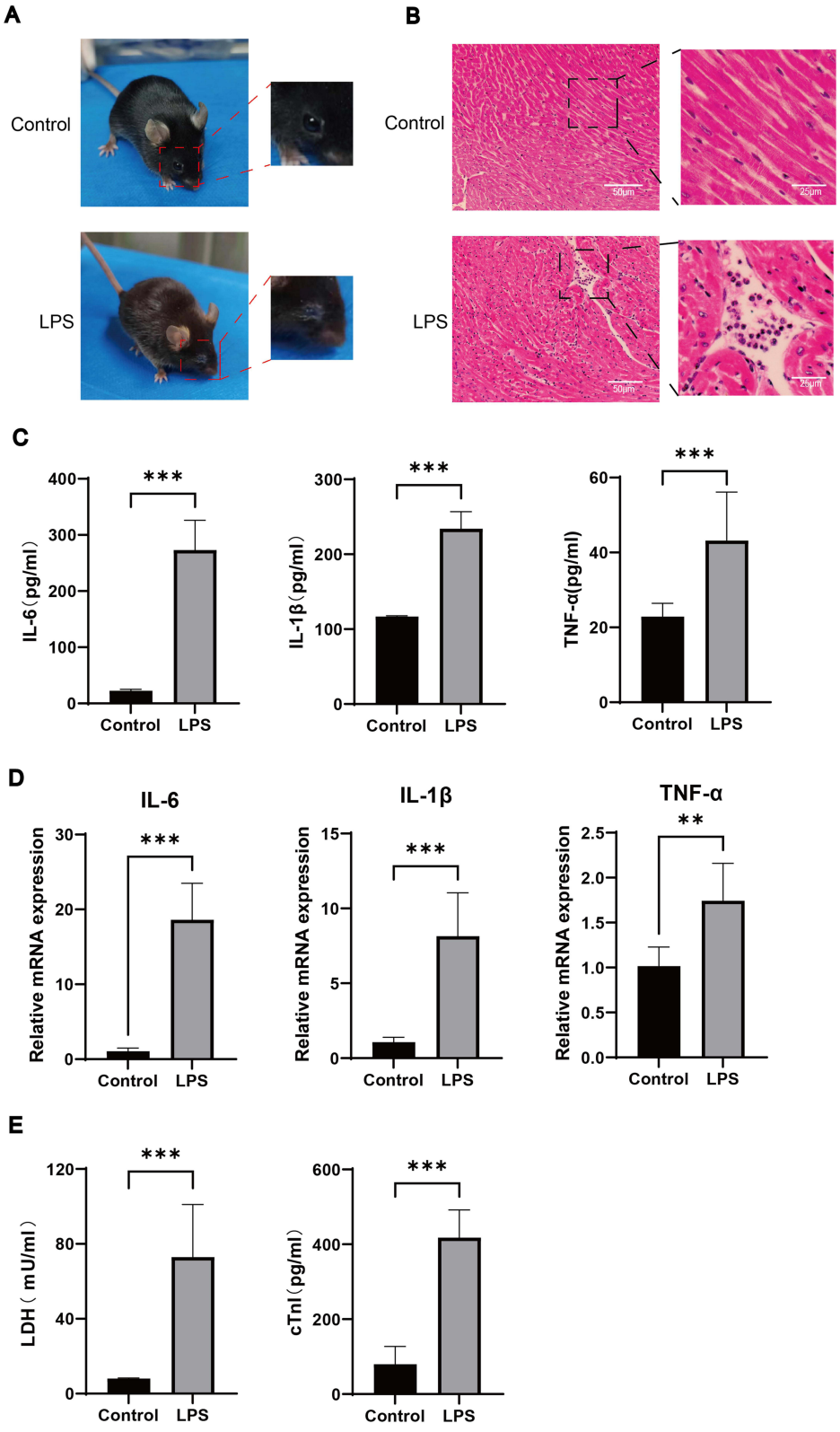

Figure 1 Septic myocardial injury mouse model; (**A**) Observation of septic myocardial injury in mice; (**B**) HE staining observation of mouse cardiac tissue; (**C**) RT-qPCR detection of mRNA levels of inflammatory factors IL-1β, IL-6, and TNF-α in mouse cardiac tissue; (**D**) ELISA detection of levels of inflammatory factors IL-1β, IL-6, and TNF-α in mouse serum; (**E**) ELISA detection of levels of myocardial injury markers LDH and cTnI in mouse serum. (**P<0.01; ***P<0.001).

 https://doi.org/10.2147/JIR.S495987

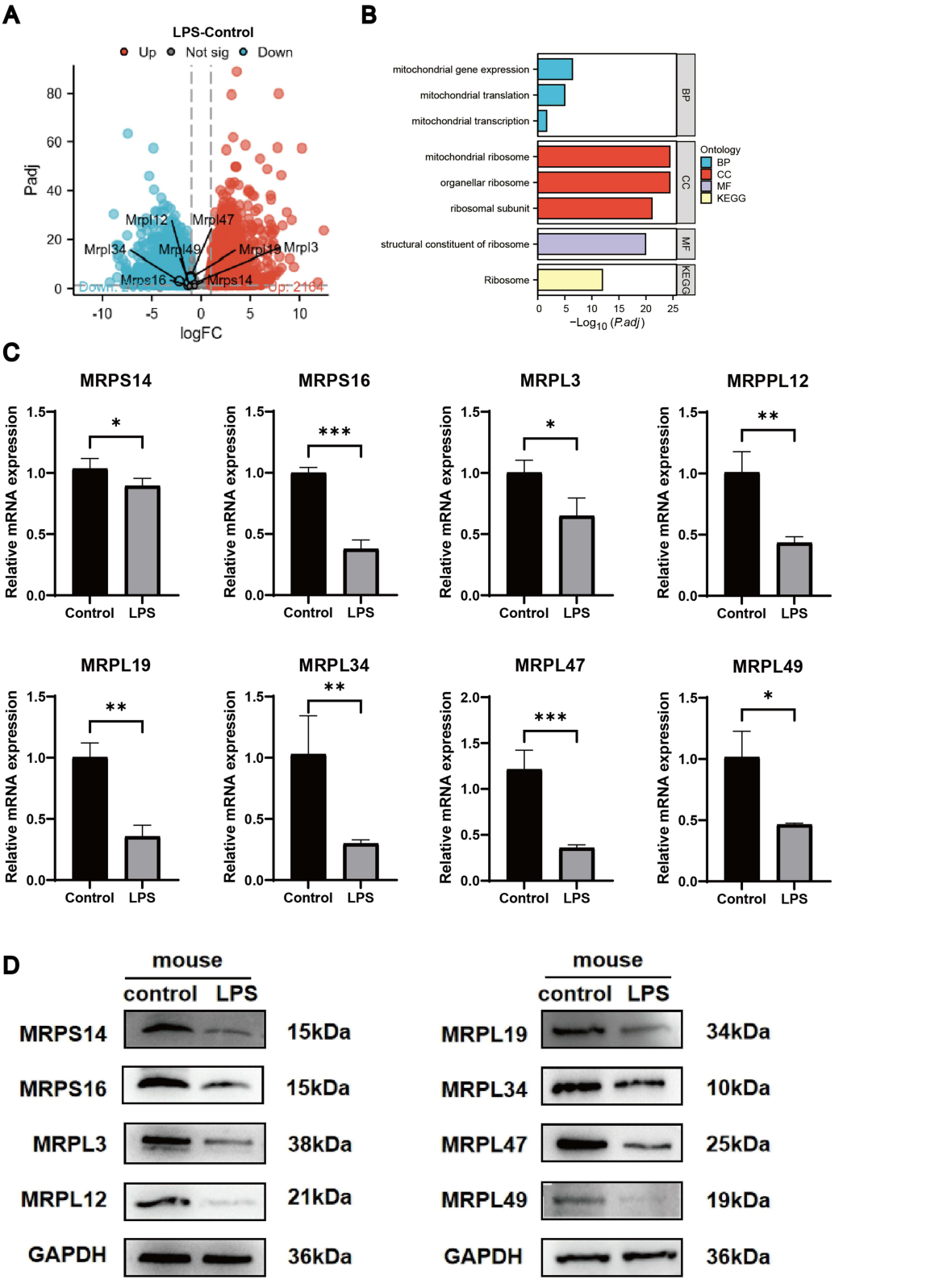

Figure 2 MRPs expression levels in mice with septic myocardial injury; (**A**) Differentially expressed gene volcano map. (**B**) GO enrichment analysis and KEGG enrichment analysis of differential genes; (**C**) RT-qPCR assay for mouse heart tissue mRNA levels of MRPs. (**D**) Western blot detection of MRPs proteins expression in mouse heart tissue. GAPDH was used as internal reference. (*P<0.05; **P<0.01; ***P<0.001).

https://doi.org/10.2147/JIR.S495987

MRPL34, MRPL47, MRPL49) were also reduced in the heart tissues of the experimental group compared with the control group (Figure 2D), confirming that MRPs were significantly under expressed in septic myocardial injury mice.

Construction of Cell Model of Septic Myocardial Injury

LPS and Nigericin were used to construct a cell model of septic myocardial injury, and the concentration and time of cell survival at around 60% were chosen as the modeling conditions for the experimental group. CCK8 results showed that LPS and Nigericin reduced the viability of AC16 cells in a dose and time dependent manner, and the cell viability of AC16 cells was around 60% when the cardiomyocytes were treated with 10 μM Nigericin for 24h or 1 μM Nigericin for 48h (Figure 3A). However, due to the long stimulation time of 48 h, the combined treatment of cardiomyocytes with 10 μg/mL LPS and 10 μM Nigericin for 24h was chosen as the condition for the subsequent experiments. After drug treatment, it was observed microscopically that cardiomyocytes increased in size and became irregular in morphology (Figure 3B). To further verify whether the septic myocardial injury cell model was constructed successfully, inflammation and myocardial injury marker assays were tested. RT-qPCR results showed that the expression levels of IL-6, IL-1β, and TNF-α mRNA were significantly higher in cardiomyocytes of the experimental group (experiment) compared with the control (Control) group (Figure 3C). ELISA The results showed that the expression levels of LDH and cTnI were significantly higher in the culture supernatants of AC16 cardiomyocytes in the experimental group (experiment) compared with the control group (Figure 3D), suggesting that the drug successfully induced inflammation and injury in cardiomyocytes, indicating the successful construction of septic cardiomyocyte model.

Mitochondrial Ribosomal Proteins are Lowly Expressed in a Cell Model of Septic Myocardial Injury

After successful modeling, the above MRPs were validated in the cell model using RT-qPCR and Western blot. RT-qPCR results showed that the mRNA expression levels of cardiac tissue MRPs (MRPS14, MRPS16, MRPL3, MRPL12, MRPL47, MRPL49) were reduced in the experimental group compared with the control group (Figure 3E). Western blot results showed that the protein expression levels of cardiac tissue MRPs (MRPS14, MRPS16, MRPL3, MRPL12, MRPL34, MRPL47, MRPL49) were reduced in the experimental group compared with the control group (Figure 3F). Among them, MRPS16 and MRPL47 showed the most significant reduction in expression levels, and therefore, these two MRPs were selected for subsequent transfection experiments.

Successfully Constructed MRPS16 and MRPL47 Overexpression and Knockdown Cell Models and Verified Their Biological Functions

Next, MRPS16 and MRPL47, which have the largest expression differences, were selected to further investigate the biological functions played by MRPs in septic myocardial injury. The models of MRPS16 and MRPL47 overexpression and knockdown were constructed by plasmid transfection of cells, respectively. After plasmid transfection of cells, fluorescence microscopy was used to observe whether the cells showed green fluorescence to initially determine the transfection efficiency. The number of cells emitting fluorescence and the total number of cells were counted in multiple fields of view, and then the transfection efficiency was expressed as the percentage of the number of cells emitting fluorescence to the total number of cells can be transfection efficiency. During transfection, effects on cell viability are unavoidable. During the pre-experiment we observed that the transfection reagent lipo3000 did inhibit cell viability. However, there was no significant difference in cell viability between the negative control transfection group and the plasmid transfection group, which led to the consistency of the cell number between the experimental group and the control group after transfection, and laid the foundation for the accuracy and reliability of the subsequent experiments. The results showed that the transfection efficiency of the overexpression and knockdown plasmids was around 80% after 24h of transfection (Figure 4A and B), indicating that both the overexpression and knockdown plasmids were successful in transfecting AC16 cells. Then RT-qPCR and Western blot were utilized to further evaluate the transfection effect. RT-qPCR results showed that compared with the overexpression control group, the RNA levels in the Ov-MRPS16 and Ov-MRPL47 groups were significantly higher (Figure 4C), and compared with the knockdown control group, the RNA levels

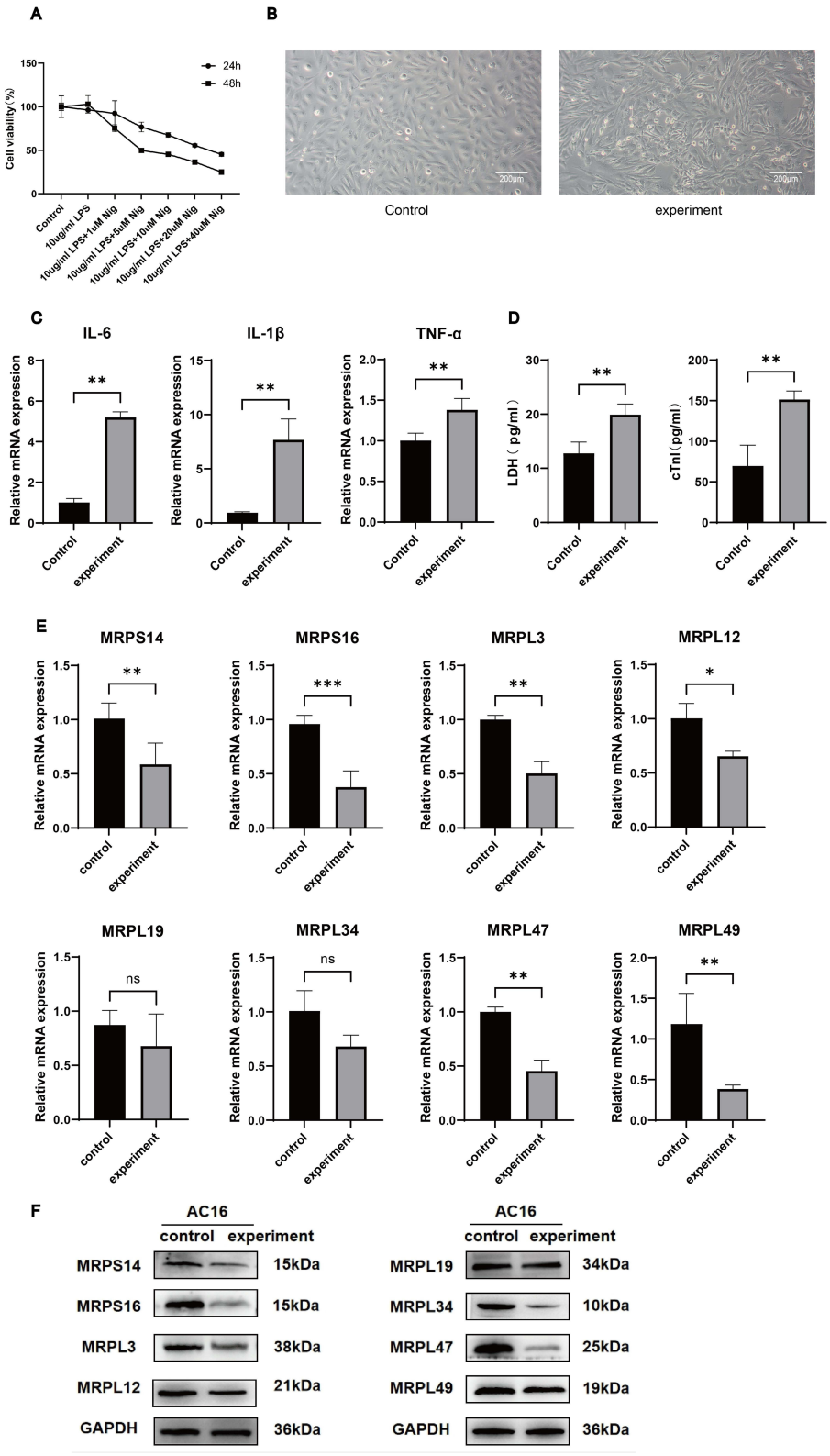

Figure 3 Septic myocardial injury cell model; (**A**) Effect of LPS and Nigericin on the viability of AC16 cells; (**B**) Morphological observation of AC16 cells; (**C**) RT-qPCR to detect the levels of inflammatory factors IL-1β, IL-6 and TNF-α mRNA in AC16 cells; (**D**) ELISA to detect the levels of cardiac injury markers cTnI and LDH levels; (**E**) RT-qPCR to detect MRPs mRNA levels in AC16 cells; (**F**) Western blot to detect MRPs protein expression in AC16 cells. (*P<0.05; **P<0.01; ***P<0.001).

https://doi.org/10.2147/JIR.S495987

in the sh-MRPS16 and sh-MRPL47 groups were significantly lower in the sh-MRPS16 and sh-MRPL47 groups compared with the overexpression control group (Figure 4D). Western blot results showed that the protein levels were significantly higher in the Ov-MRPS16 and Ov-MRPL47 groups compared with the overexpression control group (Figure 4E). Compared with the knockdown control group, the knockdown effect was observed in the sh-MRPS16-1/-2/-3 group and the sh-MRPL47-1/-2/-3 group, with the sh-MRPL47-1 group had the best

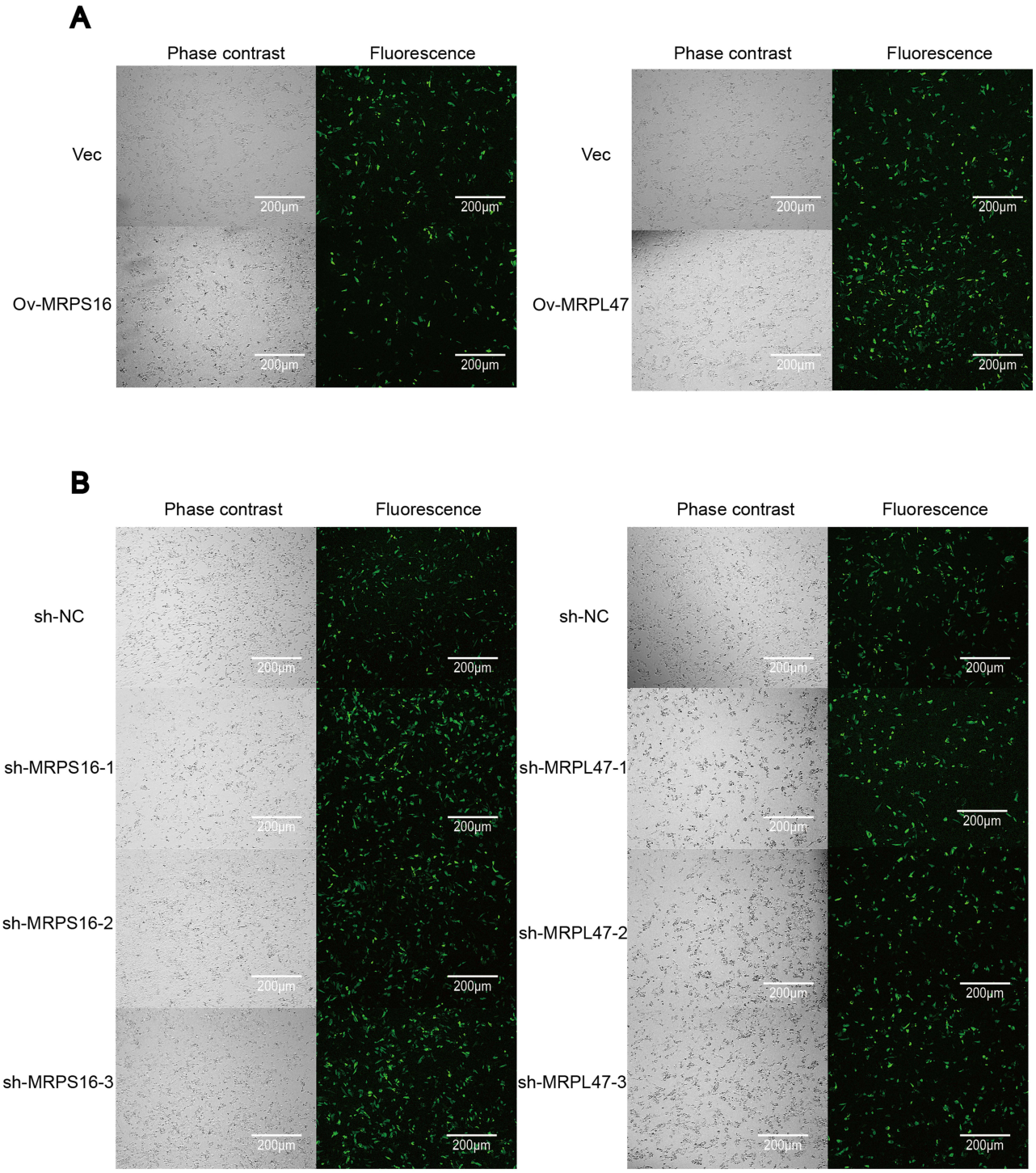

Figure 4 Continued.

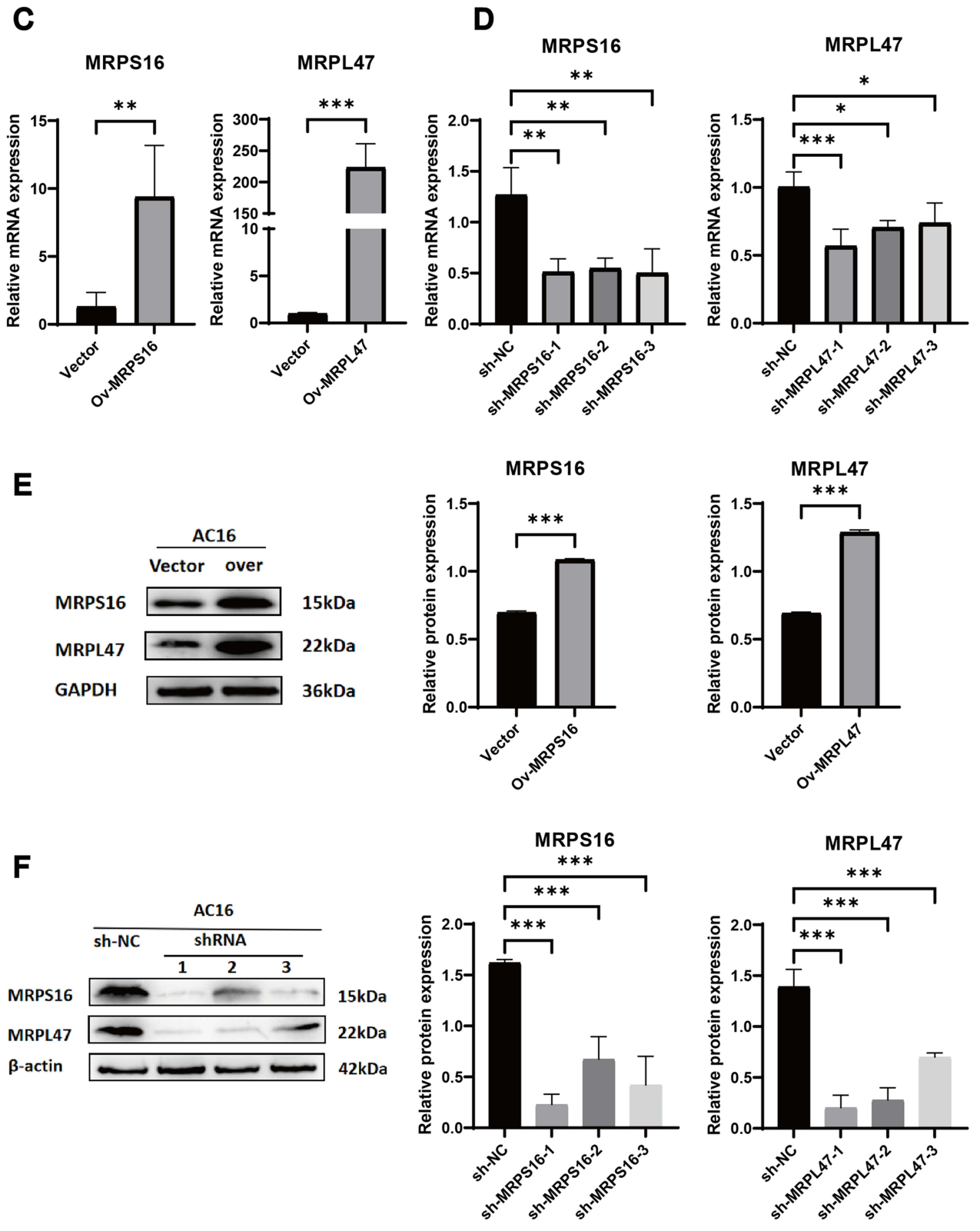

Figure 4 Plasmid-transfected cells to construct cell models of MRPS16 and MRPL47 overexpression and knockdown; (**A**) Fluorescence of MRPS16 and MRPL47 overexpression plasmid transfection under fluorescence microscope, respectively; (**B**) Fluorescence of MRPS16 and MRPL47 knockdown plasmid transfection under fluorescence microscope, respectively; (**C**) RT-qPCR to detect MRPS16 and MRPL47 overexpression mRNA effect; (**D**) RT-qPCR to detect the effect of MRPS16 and MRPL47 knockdown mRNA; (**E**) Western blot to detect the effect of MRPS16 and MRPL47 overexpressed proteins; (**F**) Western blot to detect the effect of MRPS16 and MRPL47 knockdown proteins. (*P<0.05; **P< 0.01; ***P<0.001).

https://doi.org/10.2147/JIR.S495987

knockdown effect, which was used for the follow-up study (Figure 4F), which was consistent with the RT-qPCR results, and further successfully verified the effect of transfection as well as the gene expression after transfection, and successfully constructed the MRPS16 and MRPL47 overexpression and knockdown cell models.

Both MRPS16 and MRPL47 Overexpression Alleviates Mitochondrial Biosynthesis Dysfunction Induced by Septic Myocardial Injury

After constructing overexpression and knockdown plasmids in AC16 cells, drug treatment was performed to construct septic myocardial injury cell model constructs, and the expression level of Cytochrome C Oxidase Subunit I (CO I) or PGC-1α (peroxisome proliferator-activated receptor-gamma coactivator-1α) was used to reflect mitochondrial biosynthesis. The results are shown in Figure 5A and B. mRNA levels of CO I and PGC-1α were reduced in the LPS and Nigericin treated groups compared with the normal control group, suggesting that septic myocardial injury impairs cell mitochondrial biosynthesis capacity, leading to mitochondrial dysfunction. Compared with the overexpression negative control spiking group, both CO I and PGC-1α levels were significantly increased after MRPS16 and MRPL47 overexpression. CO I and PGC-1α levels were significantly reduced after MRPS16 and MRPL47 knockdown compared to the knockdown negative control plus group. It is suggested that MRPS16 and MRPL47 overexpression can alleviate mitochondrial biosynthesis dysfunction caused by septic myocardial injury and mitigate mitochondrial damage, whereas MRPS16 and MRPL47 knockdown produces the opposite effect.

Both MRPS16 and MRPL47 Overexpression Alleviates ROS Elevation Induced by Septic Myocardial Injury

The results of flow cytometry are shown in Figure 5C, where ROS levels were significantly increased in the LPS and Nigericin treated group compared with the normal control group. Compared with the overexpression negative control spiked group, ROS levels were significantly reduced after MRPS16 overexpression and slightly reduced after MRPL47 overexpression. Compared with the knockdown negative control plus group, ROS levels were significantly elevated after MRPS16 knockdown and enhanced after MRPL47 knockdown. It is suggested that both MRPS16 and MRPL47 overexpression can alleviate the elevated ROS caused by septic myocardial injury and attenuate the mitochondrial injury, whereas MRPS16 and MRPL47 knockdown produce opposite effects.

Both MRPS16 and MRPL47 Overexpression Alleviates the Decrease in Mitochondrial Membrane Potential Induced by Septic Myocardial Injury

As shown in Figure 5D, the fluorescence intensity of mitochondrial membrane potential was significantly weakened in the LPS and Nigericin treated group compared with the normal control group. Compared with the overexpression negative control spiked group, the fluorescence intensity of mitochondrial membrane potential was significantly enhanced by MRPS16 overexpression, and the fluorescence intensity of mitochondrial membrane potential was enhanced by MRPL47 overexpression. On the contrary, the fluorescence intensity of mitochondrial membrane potential was significantly reduced after MRPS16 knockdown, and after MRPL47 knockdown, compared with the knockdown negative control addition group. It is suggested that both MRPS16 and MRPL47 overexpression can alleviate the reduction of mitochondrial membrane potential induced by septic myocardial injury, whereas MRPS16 and MRPL47 knockdown exacerbates the reduction of mitochondrial membrane potential induced by septic myocardial injury.

Both MRPS16 and MRPL47 Overexpression Alleviates the Decrease in ATP Content Induced by Septic Myocardial Injury

As shown in Figure 5E, ATP content was significantly reduced in the LPS and Nigericin treated group compared with the normal control group. Compared with the overexpression negative control spiked group, ATP content was restored after MRPS16 overexpression and increased after MRPL47 overexpression. In contrast, ATP content was reduced after MRPS16 knockdown and also after MRPL47 knockdown compared to the knockdown negative control plus group. It is suggested that both MRPS16 and MRPL47 overexpression can alleviate the decrease in ATP content caused by septic

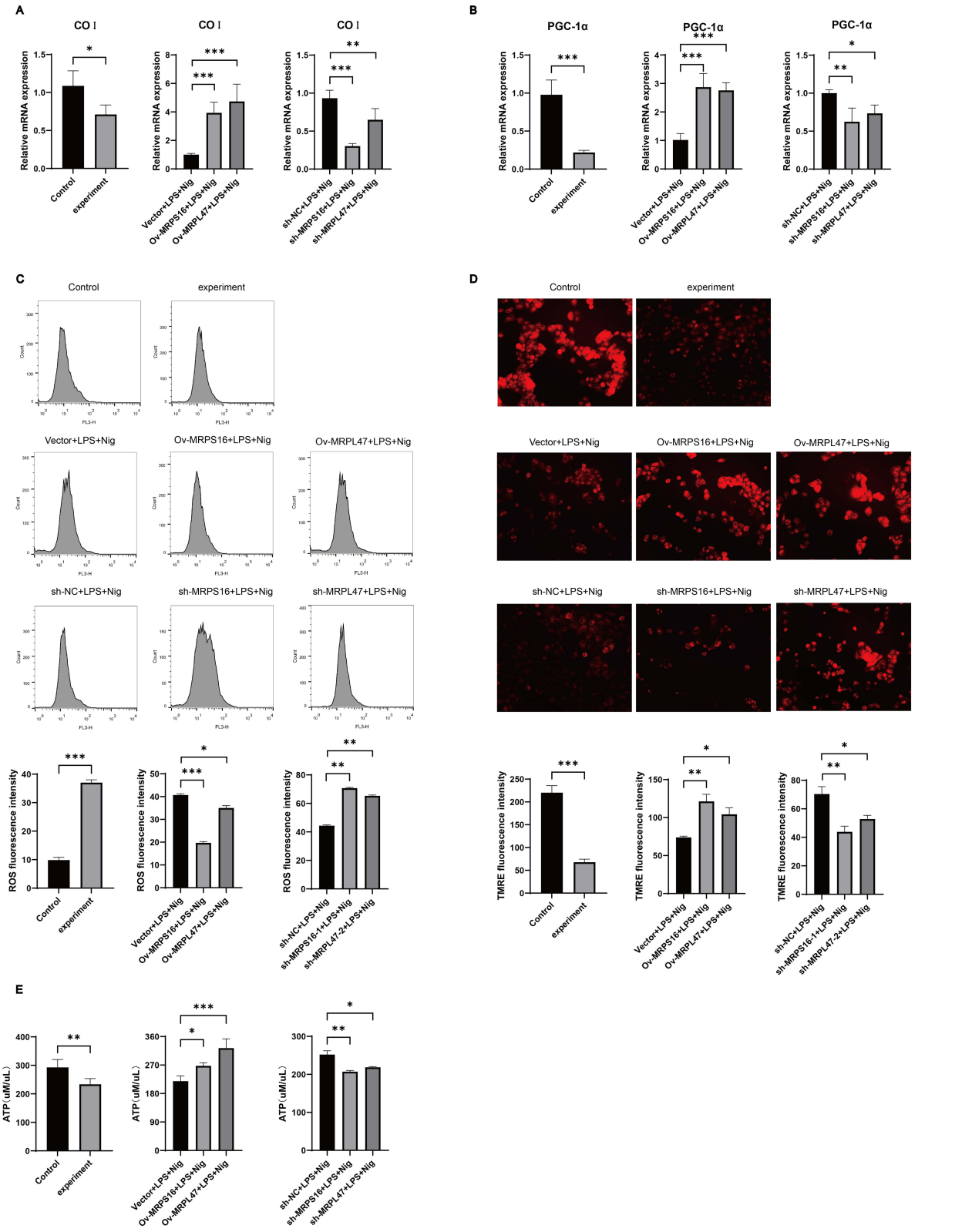

Figure 5 Effects of overexpression/knockdown in AC16 cells on mitochondrial function after constructing overexpression and knockdown septic myocardial injury cell models; (**A**) RT-qPCR to detect the expression level of CO I mRNA in AC16 cells; (**B**) RT-qPCR to detect the expression level of PGC-1α mRNA in AC16 cells; (**C**) Flow cytometry to detect the fluorescence intensity of ROS in AC16 cells; (**D**) Fluorescence microscopy to detect the fluorescence intensity of mitochondrial membrane potential of AC16 cells; (**E**) enzyme labeling to detect the ATP content of AC16 cells. (*P<0.05; **P< 0.01; ***P<0.001).

https://doi.org/10.2147/JIR.S495987

myocardial injury and ameliorate mitochondrial injury, while MRPS16 and MRPL47 knockdown exacerbate the decrease in ATP content caused by septic myocardial injury and aggravate mitochondrial injury.

Both MRPS16 and MRPL47 Overexpression Reduces Cell Pyroptosis Induced by Septic Myocardial Injury

RT-qPCR results are shown in Figure 6A, IL-1β mRNA expression levels were significantly higher in the LPS and Nigericin treated group compared to the normal control group. Compared with the overexpression negative control spiked group, IL-1β mRNA expression level was reduced after MRPS16 overexpression, and after MRPL47 overexpression, IL-1β mRNA expression level was also reduced. On the contrary, compared with the knockdown negative control addition group, IL-1βmRNA expression level was increased after MRPS16 knockdown, and IL-1βmRNA

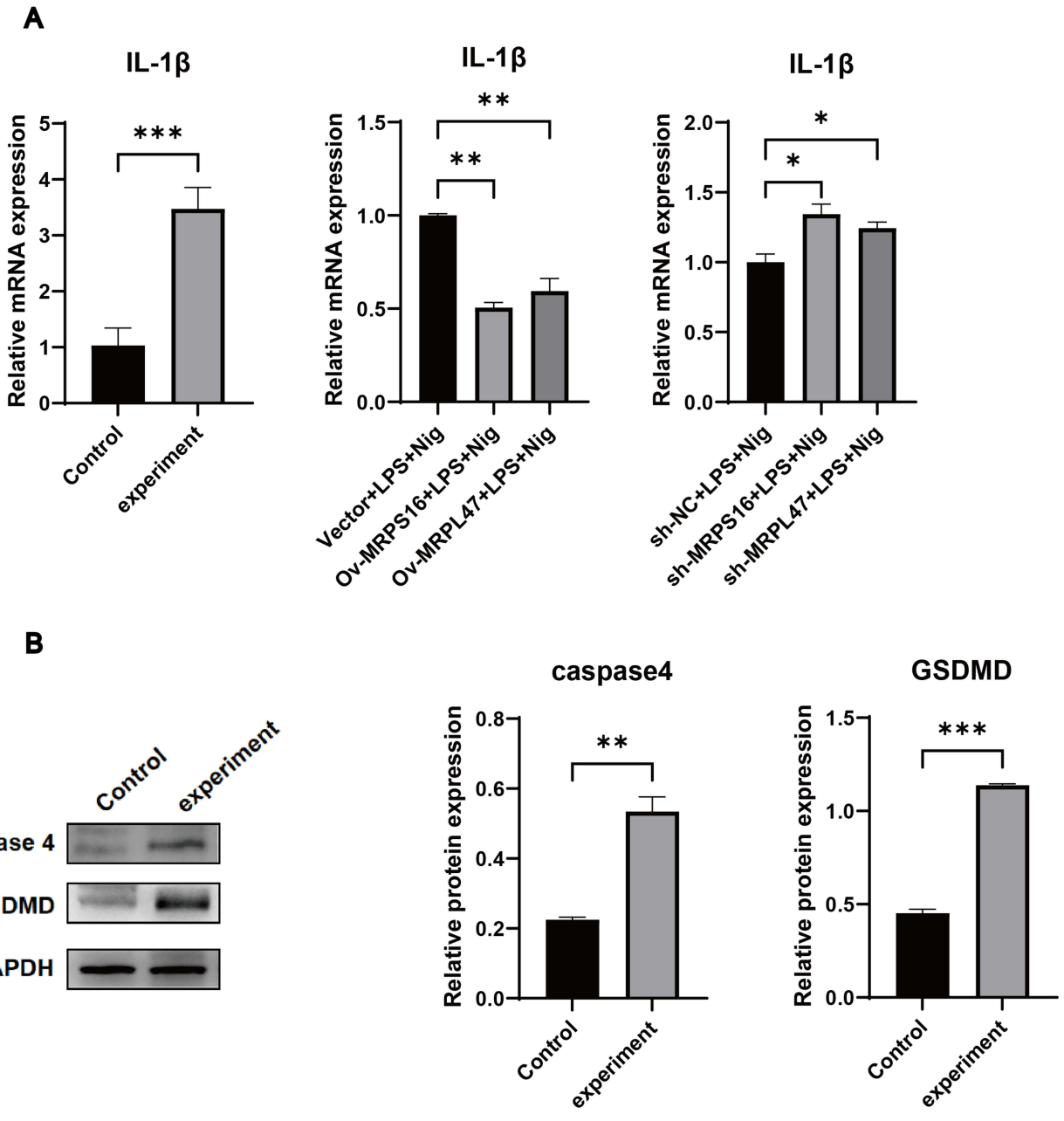

Figure 6 Continued.

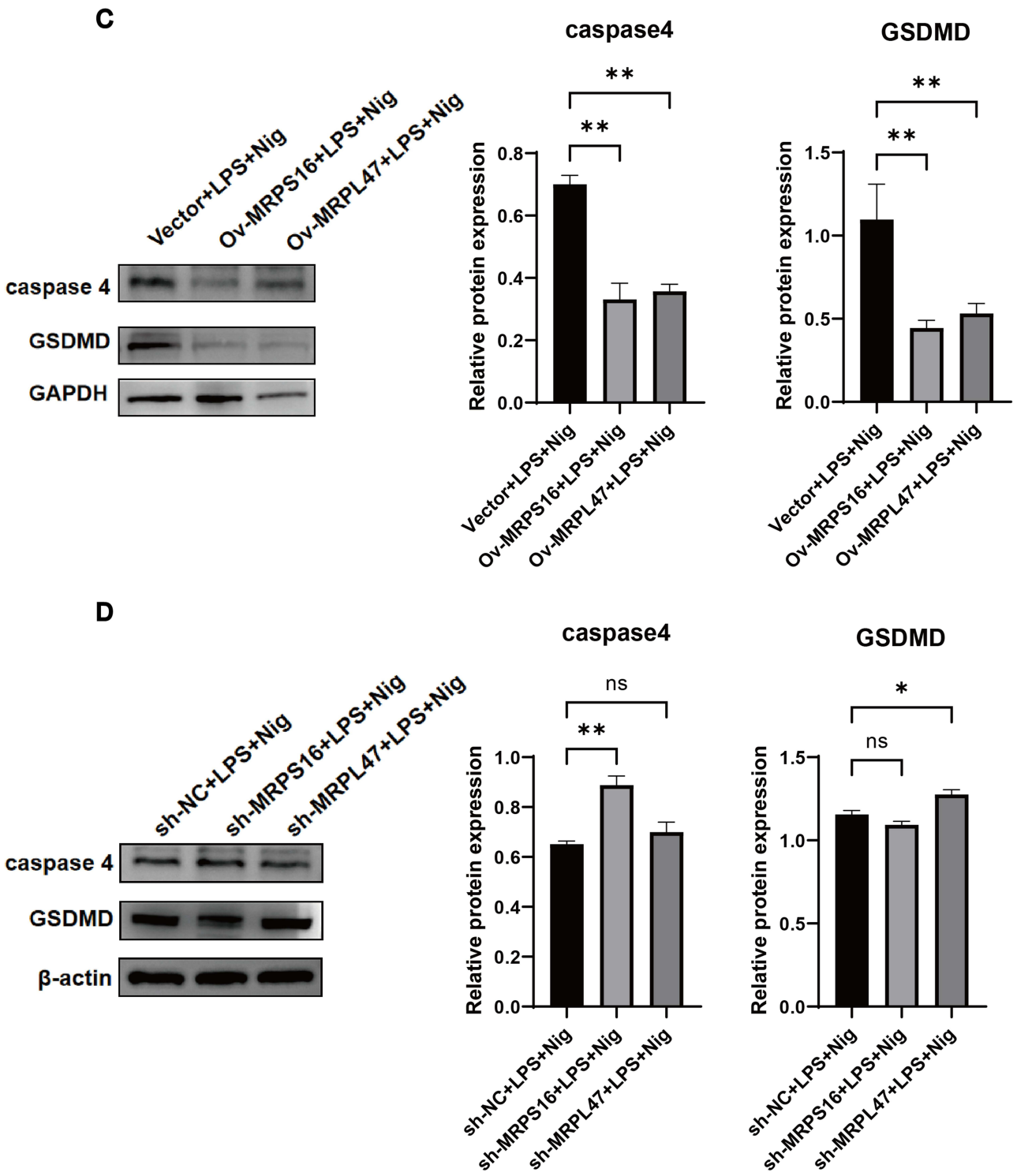

Figure 6 Effect of AC16 cells on focal death after constructing overexpression and knockdown septic myocardial injury cell models; (**A**) RT-qPCR to detect the expression level of IL-1β mRNA in AC16 cells; (**B**) Western blot to detect the expression level of caspase-4 and GSDMD in Control and experimental groups; (**C**) Western blot to detect the expression levels of caspase-4 and GSDMD in MRPS16 and MRPL47 overexpression septic myocardial injury group; (**D**) Western blot to detect the expression levels of caspase-4 and GSDMD in MRPS16 and MRPL47 knockdown septic myocardial injury group. (*P<0.05; **P< 0.01; ***P<0.001).

expression level was mildly increased after MRPL47 knockdown. Western blot results were shown in Figure 6B–D, compared with the normal control group, cardiomyocyte caspase-4, GSDMD protein expression in the addition group were all Compared with the normal control group, the caspase-4 and GSDMD protein expression of cardiomyocytes in

https://doi.org/10.2147/JIR.S495987

the drug-added group were significantly increased, suggesting that the septic myocardial injury model could cause the increase of cardiomyocyte caspase-4 and GSDMD production and promote the occurrence of nonclassical death. Compared with the overexpression-negative control plus group, caspase-4 and GSDMD expression levels were reduced after MRPS16 overexpression and MRPL47 overexpression. Compared with the knockdown negative control plus group, after MRPS16 knockdown, caspase-4 was elevated, and there was no significant change in the reduced level of GSDMD expression. After MRPL47 knockdown, there was no significant change in the level of caspase-4 expression, and there was an increase in the level of GSDMD expression, suggesting that the overexpression of MRPS16 and MRPL47 attenuates nonclassical scorched death in septic cardiomyocytes.

Discussion

Sepsis often involves multiple organs and systems, of which the heart, as an important part of the body's circulatory system, is more susceptible to sepsis damage. Septic myocardial injury can lead to cardiac insufficiency and cardiovascular failure, resulting in poor blood perfusion and even death.[35] Currently, among the determinants for evaluating animal models of sepsis, echocardiography is considered to be the most visual evidence for detecting sepsis combined with myocardial injury. Echocardiography can detect and calculate end-systolic and end-diastolic volumes, left ventricular internal diameter shortening fraction, and ejection fraction. Our group has already done echocardiography on LPS intraperitoneally injected mice, and the results showed that the LV end-diastolic internal diameter and LV end-systolic internal diameter of the LPS injected mice were significantly shortened, and the LV ejection fraction was significantly reduced, which proved that myocardial dysfunction did occur in the LPS group of mice.[36] The present study continues the previous study of LPS abdominal mice. In this study, we continued the previous modeling method of intraperitoneal injection of LPS and did not repeat the echocardiographic testing, but only evaluated the sepsis model in terms of the state of the mice, pathological HE sections, expression of inflammatory factors, and expression of markers of myocardial injury, which matched the results of the previous echocardiography. Therefore, even without echocardiography, we can assess the success of the sepsis model by observing the status of the mice, pathohistologic HE stained sections, expression of inflammatory factors, and expression of markers of myocardial injury, which will provide a simpler method for future sepsis studies.

MRPs are important for the synthesis of mitochondria-encoded proteins and maintenance of mitochondrial function. Their aberrant expression or dysfunction can lead to mitochondrial dysfunction and cell death, which are closely associated with the onset and progression of many diseases.[37] MRPS16 mutation[19] and MRPS22 mutation[20] lead to mitochondrial respiratory chain defects. In addition to mitochondrial diseases, some MRPs are abnormally expressed in tumors and may be targeted for tumor treatment. Mitochondria with normal expression of MRPs are essential for maintaining cardiac function. Abnormal expression of MRPs also contributes to heart disease, including hypertrophic cardiomyopathy and blood clots. Mitochondrial biology plays a critical role in cardiovascular disease, as mitochondria are central to cellular energy metabolism, redox balance, and apoptotic signaling, all of which are essential for maintaining cardiovascular health. The current understanding emphasizes that mitochondrial dysfunction is a hallmark of many forms of cardiovascular disease, including ischemic heart disease,[38] heart failure,[39,40] and arrhythmias.[41]

In this study, we combined the expression of MRPs in animal and cell models of septic myocardial injury and screened MRPS16 and MRPL47 for subsequent studies. The MRPS16 gene belongs to the family of ribosomal proteins MRPs, encoding 28S small subunit proteins, with a chromosomal localization of 10q22.1[a,b]-q22.2[d].[42] MRPS16 encodes a 137 amino acid protein that is one of the most conserved ribosomal proteins in mammalian and yeast mitochondria.[19] It is one of the most conserved ribosomal proteins in mammalian and yeast mitochondria. Studies have shown that MRPS16 mutations can lead to defective mitochondrial translational function and mitochondrial respiratory chain dysfunction[43] MRPS16 is commonly expressed at higher levels in tumor tissues and promotes glioma cell growth, migration, and invasion through activation of the PI3K/AKT pathway.[19] Mutations in MRPS16 have been associated with hypoplasia and malformation of the corpus callosum, as well as neonatal fatal lactic acidosis.[44] MRPS16 is highly expressed in ovarian cancer and is associated with poor prognosis.[45] MRPS16 is expressed at high levels in liver tumor cells and at lower abundance in melanoma cells. The MRPL47 gene, also a member of the MRPs family, encodes a large subunit protein and is localized to chromosome 3q26.32–3q27.1.[46] In recent years, fewer studies have been conducted on the

RPL47 gene, and mutations in the MRPL47 gene are a high risk factor for vincristine-induced peripheral neuropathy in childhood acute lymphoblastic leukemia,[47] and is also one of the differentially expressed genes detected in vitiligo,[48] at present, the role and mechanism of both MRPS16 and MRPL47 in septic myocardial injury have not been reported.

The present study demonstrated that overexpression of MRPS16 or MRPL47 could improve the mitochondrial biosynthesis dysfunction, energy metabolism disorder, and Ca^{2+} disorder caused by septic myocardial injury by reducing the decrease of CO I and PGC-1α levels, alleviating the elevation of ROS, the reduction of the mitochondrial membrane potential, and the decrease of ATP content, and thus ameliorating the mitochondrial damage caused by septic myocardial injury. In contrast, knockdown of either MRPS16 or MRPL47 resulted in a corresponding decrease in mitochondrial biosynthesis, more disturbed energy metabolism and Ca^{2+}, and aggravated cardiomyocyte injury. These results are consistent with previous studies, in which mitochondrial copy number was also increased or decreased after MRPL12 overexpression or knockdown.[49] MRPL10 knockdown decreased mitochondrial respiration and intracell ATP levels, which also led to decreased mitochondrial activity and mitochondrial complex expression.[16]

Previous studies of septic myocardial injury have focused on the regulation of apoptotic pathways by certain protein molecules or signaling pathways. For example, the protective role of PARK2/Parkin in sepsis-induced cardiac contraction and mitochondrial dysfunction.[50] Melatonin attenuates septic myocardial injury through a PI3K/Akt-dependent mechanism.[51] ZSHX regulates mitochondrial calcium homeostasis and MQS abnormalities through the TMBIM6-VDAC1 interaction mechanism, inhibiting mitochondrial damage to treat ischemic myocardial injury.[52,53] Quercetin alleviates myocardial cell injury caused by mitochondrial oxidative stress through DNA-PKcs and regulates mitosis and mitochondrial apoptosis.[54] However, our group established several animal models of sepsis heart failure including CS sepsis heart failure and LPS sepsis heart failure in the previous study, and carried out pathomorphologic observation, electron microscopic observation and apoptosis-related assays, including TUNEL apoptosis assay and apoptosis-related protein assay (Caspase3, Caspase9, Bax, Bim, Bcl2, ie), through repeated experiments, the TUNEL results all showed that apoptosis occurred in only a few sporadic cells of cardiomyocytes, which was consistent with the morphological changes observed in pathological tissue sections and electron microscopy, and the results of apoptosis-related protein assays: all suggesting that apoptosis of cardiomyocytes is not the main etiology of septic heart failure, but most likely cell pyroptosis. Currently, there are also several studies confirming that LPS-induced non-classical cell pyroptosis pathway is closely related to sepsis.[55–57] These studies suggest that pyroptosis may become an effective target for sepsis therapy in the future, providing new ideas for the prevention and treatment of diseases such as septic myocardial injury. Therefore, in the present study, we investigated the role of MRPs in cell juxtaposition by examining cell juxtaposition-related indicators (IL-1β, caspase-4, GSDMD) in overexpression and knockdown sepsis cell models. The results indicated that MRPS16 and MRPL47 could play a role in cell juxtaposition. Overexpression of MRPS16 and MRPL47 ameliorated the elevated expression levels of IL-1β, caspase-4, and GSDMD caused by septic myocardial injury, thereby alleviating the occurrence of cell juxtaposition. This may be achieved by ameliorating the mitochondrial damage. Therefore, MRPS16 and MRPL47 may be key regulatory points in regulating mitochondrial function and may serve as possible therapeutic targets for septic mitochondrial injury and septic myocardial injury.

The limitations of this study are: first, only the expression levels of MRPs in mice and AC16 cells were verified, but not further verified by clinical tissue samples. Second, the study of the mitochondrial autophagy aspect was missing in exploring the cell death mode. Third, this experiment also lacked the study of the specific pathway of action of MRPs on septic myocardial injury, which was only at the level of the effect of mitochondrial biological function. Therefore, we will continue to conduct in-depth studies in the following: first, collect myocardial tissue samples from sepsis patients to verify the expression of MRPs. Second, we will use fluorescent labeling and immunoprecipitation techniques to further explore the interaction of MRPs with key proteins and pathways of mitochondrial autophagy. Third, we will construct animal models of knockout and overexpression of MRPs to further explore the key molecular signaling pathway nodes. We will explore the specific mechanisms by which MRPs affect mitochondrial function from multiple perspectives, and lay a solid foundation for elucidating the mechanism of myocardial injury in sepsis.

Conclusion

In this study, we confirmed that MRPs (MRPS14, MRPS16, MRPL3, MRPL12, MRPL19, MRPL34, MRPL47, MRPL49) were decreased in expression in animal and cell models of septic myocardial injury. Both MRPS16 and MRPL47 overexpression could reduce mitochondrial biosynthesis dysfunction by attenuating mitochondrial biosynthesis dysfunction caused by septic myocardial injury, energy metabolism disorder and Ca^{2+} disorder, ameliorate mitochondrial injury, and thereby reduce cell pyroptosis and ultimately alleviate septic myocardial injury, Knockdown results in the opposite. Although MRPs genes have been reported in most tumors, their role in septic myocardial injury is the first time to be discovered. Meanwhile, this study preliminarily explored the potential regulatory mechanisms by which MRPS16 and MRPL47 play important roles in septic myocardial injury, which provides a possible theoretical basis for the future diagnosis and treatment of septic myocardial injury, and we will continue to conduct more in-depth analyses of potential molecular pathways by which these MRPs affect mitochondrial function in the follow-up.

Data Sharing Statement

The authors confirm that data supporting the findings of this study are available within the article.

Ethics Approval and Consent to Participant

This study was approved by the Animal Ethics Committee of the 920th Hospital of Joint Logistics Support Force of Chinese People's Liberation Army (920IEC/AF/61/2021-01.1), and followed the National Institutes of Health (NIH) Guide for the Care and Use of Laboratory Animals and the Guidelines for Chinese Regulation for the Use and Care of Laboratory Animals.

Patient Consent for Publication

Patient consent for publication was not included.

Acknowledgments

We thank the authors who contributed to the article but did not appear in the article, as well as the experimental animals who sacrificed themselves for the study.

Funding

This study was supported by was supported by the National Natural Science Foundation of China (Grant No. 81760354), Yunnan Provincial Science and Technology Department & Kunming Medical Joint Project (202201AY070001-291), the "Hundred Thousand" Project in Kunming City (2021-SW(Reserve)-70) and Health Science and Technology Project in Kunming (2023-11-01-004).

Disclosure

The authors declare no conflicts of interest.

References

1. Chacon-Cabrera A, Rojas Y, Martínez-Caro L, et al. Influence of mechanical ventilation and sepsis on redox balance in diaphragm, myocardium, limb muscles, and lungs. *Transl Res*. 2014;164(6):477–495. doi:10.1016/j.trsl.2014.07.003
2. Rudd KE, Johnson SC, Agesa KM, et al. Global, regional, and national sepsis incidence and mortality, 1990–2017: analysis for the Global Burden of Disease Study. *Lancet*. 2020;395(10219):200–211. doi:10.1016/S0140-6736(19)32989-7
3. Lin H, Wang W, Lee M, Meng Q, Ren H. Current status of septic cardiomyopathy: basic science and clinical progress. *Front Pharmacol*. 2020;11:210. doi:10.3389/fphar.2020.00210
4. Hochstadt A, Meroz Y, Landesberg G. Myocardial dysfunction in severe sepsis and septic shock: more questions than answers? *J Cardiothorac Vasc Anesth*. 2011;25(3):526–535. doi:10.1053/j.jvca.2010.11.026
5. L'heureux M, Sternberg M, Brath L, Turlington J, Kashiouris MG. Sepsis-induced cardiomyopathy: a comprehensive review. *Curr Cardiol Rep*. 2020;22(5):35. doi:10.1007/s11886-020-01277-2
6. Antonucci E, Fiaccadori E, Donadello K, Taccone FS, Franchi F, Scolletta S. Myocardial depression in sepsis: from pathogenesis to clinical manifestations and treatment. *J Crit Care*. 2014;29(4):500–511. doi:10.1016/j.jcrc.2014.03.028

7. Zeng Y, Cao G, Lin L, et al. Resveratrol attenuates sepsis-induced cardiomyopathy in rats through anti-ferroptosis via the Sirt1/Nrf2 pathway. *J Invest Surg*. 2023;36(1):2157521. doi:10.1080/08941939.2022.2157521
8. Li N, Wang W, Zhou H, et al. Ferritinophagy-mediated ferroptosis is involved in sepsis-induced cardiac injury. *Free Radic Biol Med*. 2020;160:303–318. doi:10.1016/j.freeradbiomed.2020.08.009
9. Li Z, Wu B, Chen J, et al. WWP2 protects against sepsis-induced cardiac injury through inhibiting cardiomyocyte ferroptosis. *J Transl Int Med*. 2024;12(1):35–50. doi:10.2478/jtim-2024-0004
10. Zhou B, Tian R. Mitochondrial dysfunction in pathophysiology of heart failure. *J Clin Invest*. 2018;128(9):3716–3726. doi:10.1172/JCI120849
11. Pan P, Wang X, Liu D. The potential mechanism of mitochondrial dysfunction in septic cardiomyopathy. *J Int Med Res*. 2018;46(6):2157–2169. doi:10.1177/0300060518765896
12. Shang X, Li J, Yu R, et al. Sepsis-related myocardial injury is associated with Mst1 upregulation, mitochondrial dysfunction and the Drp1/F-actin signaling pathway. *J Mol Histol*. 2019;50(2):91–103. doi:10.1007/s10735-018-09809-5
13. Greber BJ, Ban N. Structure and function of the mitochondrial ribosome. *Annu Rev Biochem*. 2016;85:103–132. doi:10.1146/annurev-biochem-060815-014343
14. Sun N, Finkel T. Cardiac mitochondria: a surprise about size. *J Mol Cell Cardiol*. 2015;82:213–215. doi:10.1016/j.yjmcc.2015.01.009
15. Xu H, Zou R, Li F, et al. MRPL15 is a novel prognostic biomarker and therapeutic target for epithelial ovarian cancer. *Cancer Med*. 2021;10(11):3655–3673. doi:10.1002/cam4.3907
16. Li HB, Wang RX, Jiang HB, et al. Mitochondrial ribosomal protein L10 associates with cyclin B1/Cdk1 activity and mitochondrial function. *DNA Cell Biol*. 2016;35(11):680–690. doi:10.1089/dna.2016.3271
17. Richman TR, Ermer JA, Davies SM, et al. Mutation in MRPS34 compromises protein synthesis and causes mitochondrial dysfunction. *PLoS Genet*. 2015;11(3):e1005089. doi:10.1371/journal.pgen.1005089
18. Lake NJ, Webb BD, Stroud DA, et al. Biallelic mutations in MRPS34 lead to instability of the small mitoribosomal subunit and Leigh syndrome. *Am J Hum Genet*. 2017;101(2):239–254. doi:10.1016/j.ajhg.2017.07.005
19. Wang Z, Li J, Long X, Jiao L, Zhou M, Wu K. MRPS16 facilitates tumor progression via the PI3K/AKT/Snail signaling axis. *J Cancer*. 2020;11(8):2032–2043. doi:10.7150/jca.39671
20. Saada A, Shaag A, Arnon S, et al. Antenatal mitochondrial disease caused by mitochondrial ribosomal protein (MRPS22) mutation. *J Med Genet*. 2007;44(12):784–786. doi:10.1136/jmg.2007.053116
21. Xu YH, Deng JL, Wang LP, et al. Identification of candidate genes associated with breast cancer prognosis. *DNA Cell Biol*. 2020;39(7):1205–1227. doi:10.1089/dna.2020.5482
22. Guo X, Lin W, Bao J, et al. A comprehensive cis-eQTL analysis revealed target genes in breast cancer susceptibility loci identified in genome-wide association studies. *Am J Hum Genet*. 2018;102(5):890–903. doi:10.1016/j.ajhg.2018.03.016
23. Wang K, Li L, Fu L, et al. Integrated bioinformatics analysis the function of RNA Binding Proteins (RBPs) and their prognostic value in breast cancer. *Front Pharmacol*. 2019;10:140. doi:10.3389/fphar.2019.00140
24. Zhou C, Chen Z, Peng C, Chen C, Li H. Long noncoding RNA TRIM52-AS1 Sponges miR-514a-5p to facilitate hepatocellular carcinoma progression through increasing MRPS18A. *Cancer Biother Radiopharm*. 2021;36(2):211–219. doi:10.1089/cbr.2019.3271
25. Sultana N, Rahman M, Myti S, Islam J, Mustafa MG, Nag K. A novel knowledge-derived data potentizing method revealed unique liver cancer-associated genetic variants. *Hum Genomics*. 2019;13(1):30. doi:10.1186/s40246-019-0213-7
26. Pu M, Wang J, Huang Q, et al. High MRPS23 expression contributes to hepatocellular carcinoma proliferation and indicates poor survival outcomes. *Tumour Biol*. 2017;39(7):1010428317709127. doi:10.1177/1010428317709127
27. Huang G, Li H, Zhang H. Abnormal expression of mitochondrial ribosomal proteins and their encoding genes with cell apoptosis and diseases. *Int J Mol Sci*. 2020;21(22):8879. doi:10.3390/ijms21228879
28. Meng Z, Chen C, Cao H, Wang J, Shen E. Whole transcriptome sequencing reveals biologically significant RNA markers and related regulating biological pathways in cardiomyocyte hypertrophy induced by high glucose. *J Cell Biochem*. 2019;120(1):1018–1027. doi:10.1002/jcb.27546
29. Jackson CB, Huemer M, Bolognini R, et al. A variant in MRPS14 (uS14m) causes perinatal hypertrophic cardiomyopathy with neonatal lactic acidosis, growth retardation, dysmorphic features and neurological involvement. *Hum Mol Genet*. 2019;28(4):639–649. doi:10.1093/hmg/ddy374
30. Carroll CJ, Isohanni P, Pöyhönen R, et al. Whole-exome sequencing identifies a mutation in the mitochondrial ribosome protein MRPL44 to underlie mitochondrial infantile cardiomyopathy. *J Med Genet*. 2013;50(3):151–159. doi:10.1136/jmedgenet-2012-101375
31. Galmiche L, Serre V, Beinat M, et al. Exome sequencing identifies MRPL3 mutation in mitochondrial cardiomyopathy. *Hum Mutat*. 2011;32(11):1225–1231. doi:10.1002/humu.21562
32. Kang K, Li J, Li R, et al. Potentially critical roles of NDUFB5, TIMMDC1, and VDAC3 in the progression of septic cardiomyopathy through integrated bioinformatics analysis. *DNA Cell Biol*. 2020;39(1):105–117. doi:10.1089/dna.2019.4859
33. Serre V, Rozanska A, Beinat M, et al. Mutations in mitochondrial ribosomal protein MRPL12 leads to growth retardation, neurological deterioration and mitochondrial translation deficiency. *BBA*. 2013;1832(8):1304–1312. doi:10.1016/j.bbadis.2013.04.014
34. Adu-Amankwaah J, Adekunle AO, Tang Z, et al. Estradiol contributes to sex differences in resilience to sepsis-induced metabolic dysregulation and dysfunction in the heart via GPER-1-mediated PPARδ/NLRP3 signaling. *Metabolism*. 2024;156:155934. doi:10.1016/j.metabol.2024.155934
35. Zhou Q, Xie M, Zhu J, et al. PINK1 contained in huMSC-derived exosomes prevents cardiomyocyte mitochondrial calcium overload in sepsis via recovery of mitochondrial Ca(2+) efflux. *Stem Cell Res Ther*. 2021;12(1):269. doi:10.1186/s13287-021-02325-6
36. Yang KQ. Study on the expression changes of ribosomal proteins in septic myocardial injury. 2021.
37. Del Giudice L, Alifano P, Calcagnile M, et al. Mitochondrial ribosomal protein genes connected with Alzheimer's and tellurite toxicity. *Mitochondrion*. 2022;64:45–58. doi:10.1016/j.mito.2022.02.006
38. Rocca C, Soda T, De Francesco EM, et al. Mitochondrial dysfunction at the crossroad of cardiovascular diseases and cancer. *J Transl Med*. 2023;21(1):635. doi:10.1186/s12967-023-04498-5
39. Liu M, Lv J, Pan Z, Wang D, Zhao L, Guo X. Mitochondrial dysfunction in heart failure and its therapeutic implications. *Front Cardiovasc Med*. 2022;9:945142. doi:10.3389/fcvm.2022.945142
40. Brown DA, Perry JB, Allen ME, et al. Expert consensus document: mitochondrial function as a therapeutic target in heart failure. *Nat Rev Cardiol*. 2017;14(4):238–250. doi:10.1038/nrcardio.2016.203

41. Saadeh K, Fazmin IT. Mitochondrial dysfunction increases arrhythmic triggers and substrates; potential anti-arrhythmic pharmacological targets. *Front Cardiovasc Med*. 2021;8:646932. doi:10.3389/fcvm.2021.646932
42. Sylvester JE, Fischel-Ghodsian N, Mougey EB, O'brien TW. Mitochondrial ribosomal proteins: candidate genes for mitochondrial disease. *Genet Med*. 2004;6(2):73–80. doi:10.1097/01.GIM.0000117333.21213.17
43. Emdadul Haque M, Grasso D, Miller C, Spremulli LL, Saada A. The effect of mutated mitochondrial ribosomal proteins S16 and S22 on the assembly of the small and large ribosomal subunits in human mitochondria. *Mitochondrion*. 2008;8(3):254–261. doi:10.1016/j.mito.2008.04.004
44. Miller C, Saada A, Shaul N, et al. Defective mitochondrial translation caused by a ribosomal protein (MRPS16) mutation. *Ann Neurol*. 2004;56 (5):734–738. doi:10.1002/ana.20282
45. Hao YX. A preliminary study on the expression and role of MRPL15 in epithelial ovarian tumors: a comprehensive analysis of bioinformatics and clinical samples. 2022.
46. Yang BH. Mitochondrial ribosomal proteins and mitochondrial diseases. *Chin J Eugen Genet*. 2005;2005(07):1–3.
47. Abaji R, Ceppi F, Patel S, et al. Genetic risk factors for VIPN in childhood acute lymphoblastic leukemia patients identified using whole-exome sequencing. *Pharmacogenomics*. 2018;19(15):1181–1193. doi:10.2217/pgs-2018-0093
48. Lei Z, Yu S, Ding Y, et al. Identification of key genes and pathways involved in vitiligo development based on integrated analysis. *Medicine*. 2020;99(31):e21297. doi:10.1097/MD.0000000000021297
49. Han Y, Liu Y, Zhen J, et al. P53 regulates mitochondrial biogenesis via transcriptionally induction of mitochondrial ribosomal protein L12. *Exp Cell Res*. 2022;418(1):113249. doi:10.1016/j.yexcr.2022.113249
50. Piquereau J, Godin R, Deschênes S, et al. Protective role of PARK2/Parkin in sepsis-induced cardiac contractile and mitochondrial dysfunction. *Autophagy*. 2013;9(11):1837–1851. doi:10.4161/auto.26502
51. An R, Zhao L, Xi C, et al. Melatonin attenuates sepsis-induced cardiac dysfunction via a PI3K/Akt-dependent mechanism. *Basic Res Cardiol*. 2016;111(1):8. doi:10.1007/s00395-015-0526-1
52. Chang X, Zhou S, Liu J, et al. Zishen Tongyang Huoxue decoction (TYHX) alleviates sinoatrial node cell ischemia/reperfusion injury by directing mitochondrial quality control via the VDAC1-β-tubulin signaling axis. *J Ethnopharmacol*. 2024;320:117371. doi:10.1016/j.jep.2023.117371
53. Chang X, Zhou S, Liu J, et al. Zishenhuoxue decoction-induced myocardial protection against ischemic injury through TMBIM6-VDAC1-mediated regulation of calcium homeostasis and mitochondrial quality surveillance. *Phytomedicine*. 2024;132:155331.
54. Chang X, Zhang Q, Huang Y, et al. Quercetin inhibits necroptosis in cardiomyocytes after ischemia-reperfusion via DNA-PKcs-SIRT5-orchestrated mitochondrial quality control. *Phytother Res*. 2024;38(5):2496–2517. doi:10.1002/ptr.8177
55. Hagar JA, Powell DA, Aachoui Y, Ernst RK, Miao EA. Cytoplasmic LPS activates caspase-11: implications in TLR4-independent endotoxic shock. *Science*. 2013;341(6151):1250–1253. doi:10.1126/science.1240988
56. Song F, Hou J, Chen Z, et al. Sphingosine-1-phosphate receptor 2 signaling promotes caspase-11-dependent macrophage pyroptosis and worsens Escherichia coli sepsis outcome. *Anesthesiology*. 2018;129(2):311–320. doi:10.1097/ALN.0000000000002196
57. Deng M, Tang Y, Li W, et al. The endotoxin delivery protein HMGB1 mediates caspase-11-dependent lethality in sepsis. *Immunity*. 2018;49 (4):740–753.e747. doi:10.1016/j.immuni.2018.08.016